




Measured Performance of Residential Dehumidifiers Under Cyclic Operation

J. Winkler, D. Christensen, and J. Tomerlin

NREL is a national laboratory of the U.S. Department of Energy
Office of Energy Efficiency & Renewable Energy
Operated by the Alliance for Sustainable Energy, LLC.

This report is available at no cost from the National Renewable Energy Laboratory (NREL) at www.nrel.gov/publications.

Technical Report
NREL/TP-5500-61076
January 2014

Contract No. DE-AC36-08GO28308

Measured Performance of Residential Dehumidifiers Under Cyclic Operation

J. Winkler, D. Christensen, and J. Tomerlin

Prepared under Task No. BE13.0201

NREL is a national laboratory of the U.S. Department of Energy
Office of Energy Efficiency & Renewable Energy
Operated by the Alliance for Sustainable Energy, LLC.

National Renewable Energy Laboratory
15013 Denver West Parkway
Golden, CO 80401
303-275-3000 • www.nrel.gov

Technical Report
NREL/TP-5500-61076
January 2014

Contract No. DE-AC36-08GO28308

This report is available at no cost from the National Renewable Energy Laboratory (NREL) at www.nrel.gov/publications.

Available electronically at http://www.osti.gov/bridge

Available for a processing fee to U.S. Department of Energy and its contractors, in paper, from:

U.S. Department of Energy
Office of Scientific and Technical Information
P.O. Box 62
Oak Ridge, TN 37831-0062
phone: 865.576.8401
fax: 865.576.5728
email: mailto:reports@adonis.osti.gov

Available for sale to the public, in paper, from:

U.S. Department of Commerce
National Technical Information Service
5285 Port Royal Road
Springfield, VA 22161
phone: 800.553.6847
fax: 703.605.6900
email: orders@ntis.fedworld.gov
online ordering: http://www.ntis.gov/help/ordermethods.aspx

Cover Photos: (left to right) photo by Pat Corkery, NREL 16416, photo from SunEdison, NREL 17423, photo by Pat Corkery, NREL 16560, photo by Dennis Schroeder, NREL 17613, photo by Dean Armstrong, NREL 17436, photo by Pat Corkery, NREL 17721.

Printed on paper containing at least 50% wastepaper, including 10% post consumer waste.

Executive Summary

Residential construction practices are progressing toward higher levels of energy efficiency. A proven strategy to save energy is to simultaneously increase building insulation levels and reduce outdoor air infiltration. Tight homes require intentional mechanical ventilation to ensure healthy indoor air. Overall, this strategy results in a shift in the mix of latent and sensible space conditioning loads, requiring proportionally more moisture to be removed compared to standard homes. Insufficient information is currently available at a wide enough range of operating points to design dehumidification systems for high performance homes in hot-humid climates. The only industry information available on dehumidifier moisture removal and energy consumption consists of performance ratings conducted at a single steady-state test condition, whereas these products cycle on and off when in use. To understand energy impacts associated with controlling indoor humidity to safe and comfortable levels, we need accurate numerical models and performance data for residential dehumidification equipment under both steady-state and cyclic operation.

Winkler et al. (2011) developed steady-state performance maps to predict dehumidifier performance under a variety of indoor conditions. However, installed heating, ventilating, and air-conditioning (HVAC) equipment rarely operates at steady state. Part load performance testing of residential dehumidifiers is not mandated by current test standards. Therefore, we developed a method for cyclic performance evaluation, and tested the part load performance of four residential dehumidifiers in the National Renewable Energy Laboratory's (NREL) Advanced HVAC Systems Laboratory.[1]

The part load fraction (efficiency degradation due to cycling) is dependent on the cycling rate and part load ratio (moisture load to be met divided by steady-state moisture removal rate). Part load efficiency of each dehumidifier was measured under 13 cycling scenarios, and combined with NREL field data to develop part load fraction performance curves under realistic cycling scenarios. Results from a ducted and standalone unit are shown in Figure ES-1, left and right, respectively.

[1] This laboratory is not certified for equipment ratings because its purpose is to conduct rapid equipment testing across a wide range of conditions representing real-world operation in whole buildings.

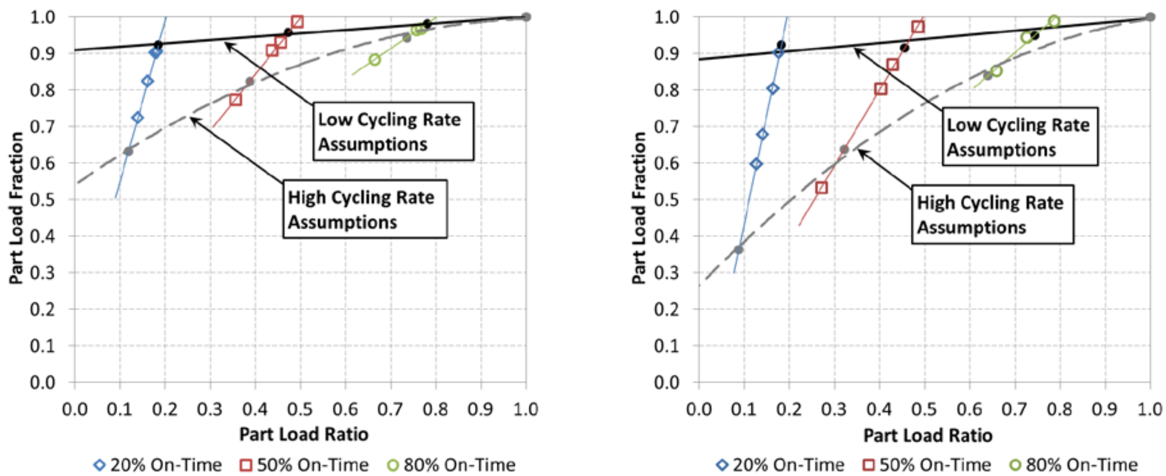

Figure ES-1. Part load efficiency degradation for a ducted dehumidifier (left) and standalone dehumidifier (right) under two cycling scenarios

Both standalone dehumidifiers operated the fan for 3 minutes after the compressor turned off, which resulted in significant latent degradation. Testing indicated that up to 42% of the moisture removed by the dehumidifier was returned to the space when compressor runtime ranged from 3–6 minutes. Thus at short runtimes, a significant portion of the energy used to dehumidify the air is wasted. Table ES-1 summarizes two control strategy improvements that would significantly improve dehumidifier part load performance.

Table ES-1. Summary of Potential Control Strategy Improvements

Recommended Control Modification	Potential Outcome	Potential Part Load Efficiency Improvement
Eliminate Extended Fan Operation	• Significantly reduce latent degradation • Reduce dehumidifier runtime by reducing moisture addition following compressor operation	Up to 20% (at high cycling rates)
Increase Dehumidistat Relative Humidity Dead Band	• Prevent dehumidifier from short cycling caused by inadequate air mixing • Encourage longer dehumidifier runtimes	Up to 30%–60% (depending on dehumidifier type)

This report, combined with the previous study (Winkler et al. 2011), provides a comprehensive dataset to accurately model residential dehumidifiers under a variety of operating conditions and part load scenarios.

Definitions

AHAM	Association of Home Appliance Manufacturers
AHRI	Air-Conditioning, Heating, and Refrigeration Institute
ANSI	American National Standards Institute
C_D	part load degradation coefficient
CDF	capacity degradation fraction
CLF	cooling load factor
CPH	cycles per hour
DB	dry-bulb
DOE	U.S. Department of Energy
DX	direct expansion
EER	energy efficiency ratio
GE	General Electric
HVAC	heating, ventilating, and air-conditioning
NREL	National Renewable Energy Laboratory
PD	pneumatically driven
PLF	part load fraction
PLR	part load ratio
RH	relative humidity
RTF	runtime fraction

Contents

List of Figures

List of Tables

1 Overview

This report details our study on cyclic performance of residential dehumidifiers. We developed a test method and apparatus to enable part load testing at the National Renewable Energy Laboratory's (NREL) Advanced Heating, Ventilating and Air-Conditioning (HVAC) Systems Laboratory.[2] Four direct-expansion (DX) dehumidifiers were tested to learn how performance degrades under a range of cycling scenarios.

When a dehumidifier cycles on, some energy is used to cool the evaporator coil, heat the condenser, and redistribute the refrigerant. Further, when the dehumidifier cycles off there will be ample condensed moisture on the evaporator coil. Energy was used to condense this humidity, and any water that re-evaporates must later be recondensed. This energy use, which does not directly result in condensed moisture, is considered a loss—it provides no benefit and does not improve occupant comfort.

Four residential dehumidifiers were tested using an NREL-developed cyclic test method, which is described in Section 2.1. Each had been previously tested at steady state, so comparison to our previous data was straightforward. Table 1 lists specifications for each unit.

Table 1. Dehumidifier Specifications

Brand Name	Model #	Capacity[a] (pints/day)	Energy Factor[a] (L/kWh)	Airflow Rate (cfm)	Type
Ultra-Aire	XT150H	150	3.7	415[b]	Ducted
Ultra-Aire	70H	70	2.32	160[b]	Ducted
General Electric (GE)	ADER65LP	65	1.8	195[c]/175/155	Standalone
Soleusair	SG-DEH-45-1	45	1.5	103[c]/91/81	Standalone

[a] Performance at the rated inlet condition of 80°F, 60% relative humidity (RH)
[b] Flow rate specified at 0 in. water gauge
[c] Cyclic testing was performed at the "high" fan speed

1.1 Motivation

Winkler et al. (2011) previously conducted laboratory performance testing of standalone and ducted residential dehumidifiers. Our objective was to develop performance maps, or detailed datasets that enable equipment simulation under any operating scenario typical to real buildings. That study was conducted for several reasons.

The Building America program—and worldwide home construction in general—are progressing toward higher and higher levels of energy efficiency. A proven strategy to save energy is to simultaneously increase building insulation levels and reduce outdoor air infiltration. Homes are being built so airtight that intentional mechanical ventilation is often required to ensure healthy

[2] This laboratory is not certified for equipment ratings because its purpose is to conduct rapid equipment testing across a wide range of conditions representing real-world operation in whole buildings.

indoor air. So although the increased enclosure insulation is significantly reducing heat gain from the warmer outdoor air, the ventilation system is bringing in some outdoor moisture (compared with the drier, air-conditioned indoor air). Overall, this results in a shift in the nature of the space conditioning loads—proportionally more moisture must be removed. Dehumidifier moisture removal and energy consumption is available at a single test condition (80°F dry-bulb (DB) and 60% RH), which is insufficient for accurately predicting dehumidifier performance in whole-building simulation tools.

Thus, our previous study developed performance data for dehumidifiers across a range of temperature and humidity. All those units were ENERGY STAR® certified under V2.0 of the dehumidifier appliance specification. Our performance data were taken at steady state, meaning the dehumidifier was operating continuously without turning on and off and had reached stable operation at the given test point. In real buildings, HVAC equipment rarely operates at steady state, so we planned the present study to understand how cycling losses affect real-world dehumidifier energy use and moisture removal.

A secondary motivation for this study was the implementation of ENERGY STAR dehumidification specification V3.0. As shown in Figure 1, this specification included a substantial increase in minimum efficiency compared to the V2.0 specification, particularly for low-capacity dehumidifiers.

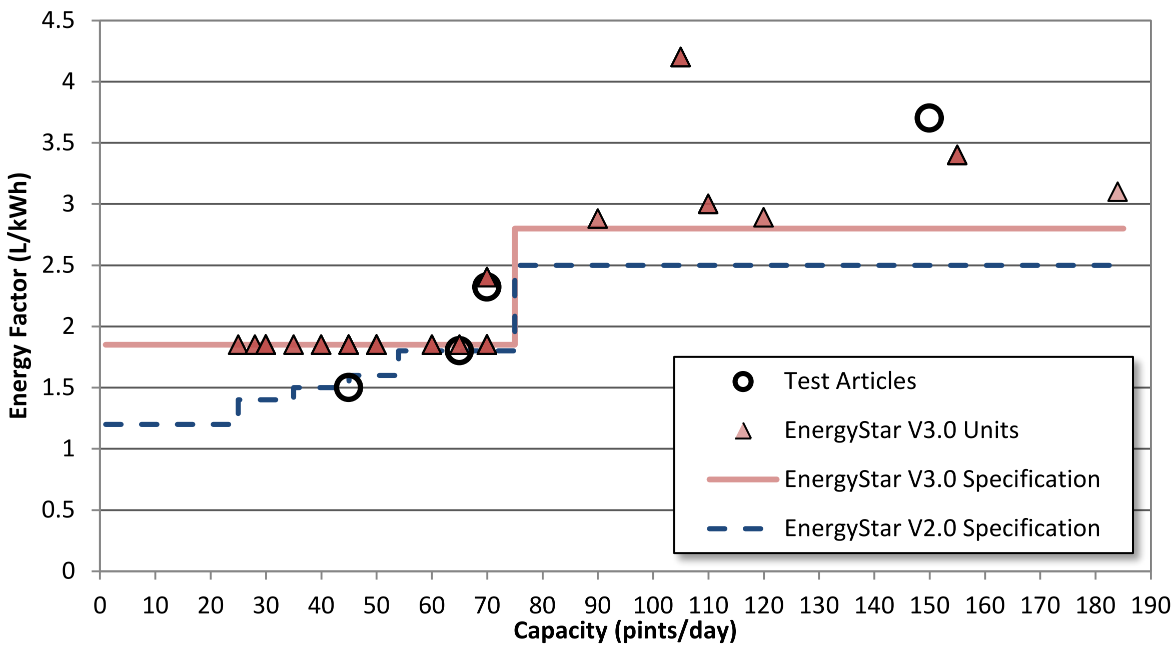

Figure 1. Capacity and energy factor for available dehumidifier products and ENERGY STAR certification requirements

Coincidentally, Fang et al. (2011) indicated smaller dehumidifiers were most appropriate for low-load homes. Thus, it seemed that owners of high performance homes might be motivated to select larger dehumidifiers certified as ENERGY STAR instead of smaller, right-sized dehumidifiers. We have interest in exploring energy-cost tradeoffs of higher efficiency operation and cycling losses for these products in order to make the best recommendations to homeowners.

After we started the present test, additional smaller capacity products that meet the ENERGY STAR V3.0 appliance efficiency requirement have entered the market. That eases the concern that consumers might be driven to oversize, but does not resolve questions about the relative benefit or cost of a more efficient but oversized dehumidifier that loses some efficiency with normal cycling operation. Additionally, the industry has not yet developed a standard dehumidifier selection procedure. Thus, in practice dehumidifiers are regularly and inadvertently oversized for the given application.

Our tests focused on the cyclic performance at conditions typically found in conditioned living space. Basement dehumidifiers tend to see cooler air with low dew point temperatures, resulting in frost formation on the evaporator coil. The dehumidifiers thus typically enter a defrost mode to remove the accumulated frost. The purpose of our experiment was to acquire the necessary data to accurately simulate the energy consumption associated with controlling living space humidity. Characterizing defrost performance was beyond the scope of the current study.

1.2 Cyclic Degradation for Air Conditioners and Heat Pumps

HVAC equipment rarely operates at steady state, but rather cycles under part load conditions to meet building loads. Under cyclic operation, the part load ratio (PLR) is defined as the ratio of the building load to the steady-state equipment capacity. At PLRs ≥ 1, the equipment runs continuously.

$$PLR = \frac{building\ load}{steady\ state\ equipment\ capacity} \tag{1}$$

Parken et al. (1977) were the first to quantify efficiency degradation for air conditioners and heat pumps caused by part load operation by developing a correlation for the part load fraction (PLF), which is defined below.

$$PLF = \frac{part\ load\ efficiency}{steady\ state\ efficiency} \tag{2}$$

Parken et al.'s approach was later adopted by the seasonal energy efficiency ratio rating procedure to determine the part load degradation coefficient (C_D). C_D calculation procedures for air conditioners and heat pumps are included in Air-Conditioning, Heating, and Refrigeration Institute (AHRI) Standard 210/240 (ANSI/AHRI 2008). For air conditioners (and heat pumps in cooling mode), C_D is calculated using performance results from a steady-state test followed by a series of on/off cycles and is a function of the energy efficiency ratio (EER) and cooling load factor (CLF).

$$C_D = \frac{1 - \frac{EER_{cyc}}{EER_{ss}}}{1 - CLF} \tag{3}$$

The CLF is equivalent to the PLR and for a cyclic test is calculated using the integrated capacity during cyclic operation:

$$CLF = \frac{q_{cyc}}{\dot{Q}_{ss} \cdot \Delta\tau_{cyc}} = \frac{\int_{t_1}^{t_2} \dot{m}_{air,evap}\left(h_{evap,in} - h_{evap,out}\right)dt}{\dot{Q}_{ss} \cdot \tau_{cyc}} \quad (4)$$

where q_{cyc} is the integrated capacity, $\dot{Q}_{ss}$ is the steady-state capacity, $\Delta\tau_{cyc}$ is the length of a cycle ($\tau_{cyc} = t_2 - t_1$), and $h_{evap,in}$ *and* $h_{evap,out}$ is air enthalpy at the inlet and outlet of the evaporator coil, respectively.

The cyclic EER is calculated using the integrated cyclic capacity and integrated power consumption during the entire on/off time period:

$$EER_{cyc} = \frac{q_{cyc}}{\int_{t_1}^{t_2} \dot{P}dt} \quad (5)$$

where $\dot{P}_{tot}$ is the instantaneous power consumption.

A correlation relating PLF to PLR is required to estimate the cyclic efficiency degradation. Rearranging Equation 3 provides a linear model for the PLF as a function PLR and C_D.

$$\frac{EER_{cyc}}{EER_{ss}} = 1 - C_D\left(1 - CLF\right) \quad (6)$$

which is equivalent to

$$PLF = 1 - C_D\left(1 - PLR\right) \quad (7)$$

Equation 7 is often used when estimating part load efficiency of air conditioners and heat pumps in building simulation tools (Henderson et al. 1999; Cutler et al. 2013) and has compared well to theoretical models (Henderson et al. 1999). However, simply using the PLR and a constant C_D value (such as in Equation 7) to estimate part load efficiency degradation fails to recognize cycling rate and on-time impacts on part load efficiency. HVAC equipment cycling rates and on-times are determined by thermostat characteristics, building thermal mass, system airflow distribution, etc. and can have a significant impact on accurately estimating the part load efficiency. Parken et al. (1977) tested air-conditioning equipment at different cycling rates and on-time fractions, but ultimately had to make assumptions about residential thermostat behavior to develop a PLF correlation. The cycling rate and on-time used in the correlation shown in Equation 7 are prescribed by AHRI Standard 210/240, which has a cycling rate of two cycles per hour (CPH) and an on-time of 6 minutes (corresponding to an off-time of 24 minutes) (ANSI/AHRI 2008). Thus, using a single C_D value to estimate part load efficiency inherently relies on the single cycle characteristics included in that test standard.

For dehumidifiers, the regulatory test method and rating standard is presently ANSI/AHAM DH-1-2008, which was adopted by the U.S. Department of Energy for regulatory purposes as United States Code of Federal Regulations, Part 430, Section 10, Subpart B, Appendix X. It specifies testing at steady state only, so no specified methods for part load estimation are available.

2 Approach

2.1 Experimental Test Procedure

NREL's Advanced HVAC Systems Laboratory is a psychrometric test facility, designed to supply air to a test article at a tightly controlled flow rate, temperature, pressure, and humidity and then measure the cooling, heating, or dehumidifying effect. This method enables rapid testing, but the laboratory systems cannot rapidly cycle on and off while sufficiently controlling the inlet condition. We developed a cycling test configuration to overcome that limitation. Figure 2 shows a schematic of the experimental configuration.

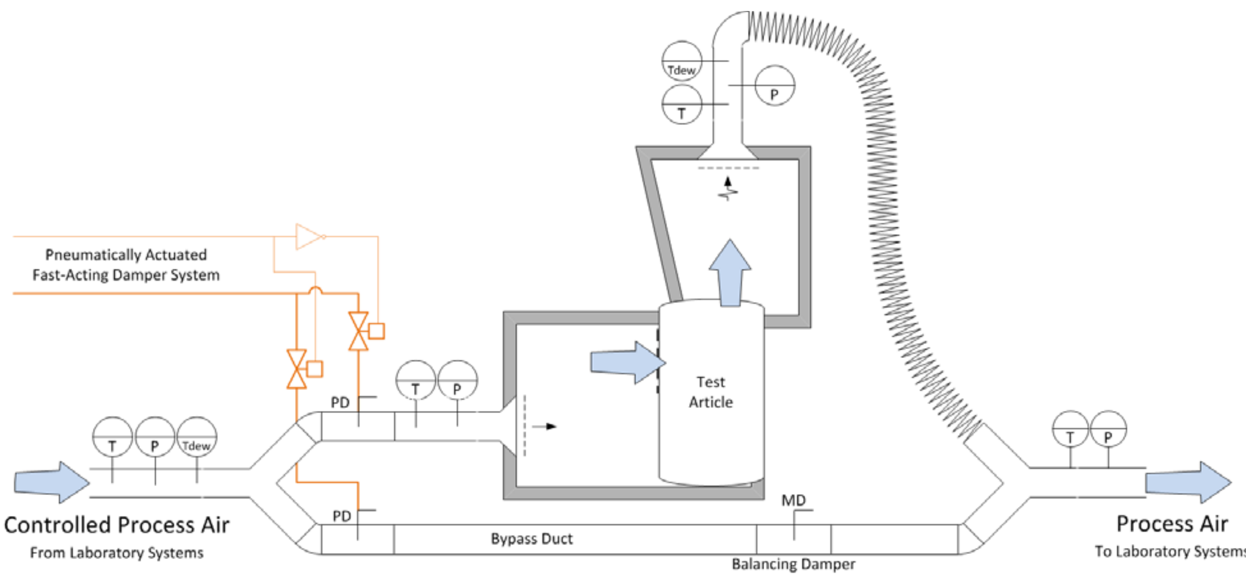

Figure 2. Schematic of the experiment configuration

A pair of pneumatically driven (PD) fast-acting sealing dampers was triggered by the data acquisition system so that when the unit's fan cycled off, process air was diverted through a bypass duct. A manual balancing damper was used to ensure the pressure regime within the laboratory systems was equivalent whether the test article was on or off.

Air temperature, pressure, flow rate, and humidity were measured on both the inlet and outlet of the test article. Along with electrical energy consumption, this enabled calculation of energy and mass balances that indicate overall measurement accuracy. All data were collected at 5 Hz and average values were stored at 1 Hz.

Winkler et al. (2011) provide additional details on NREL's Advanced HVAC Systems Laboratory and the experimental approach used to test residential dehumidifiers.

Figure 3 and Figure 4 include photographs of the Ultra-Aire 70H and GE test setups, respectively. Though the test setup was similar for both dehumidifier types, the schematic in Figure 2 directly applies to the standalone dehumidifier set (as in Figure 4). Additional photographs are included in Appendix A.

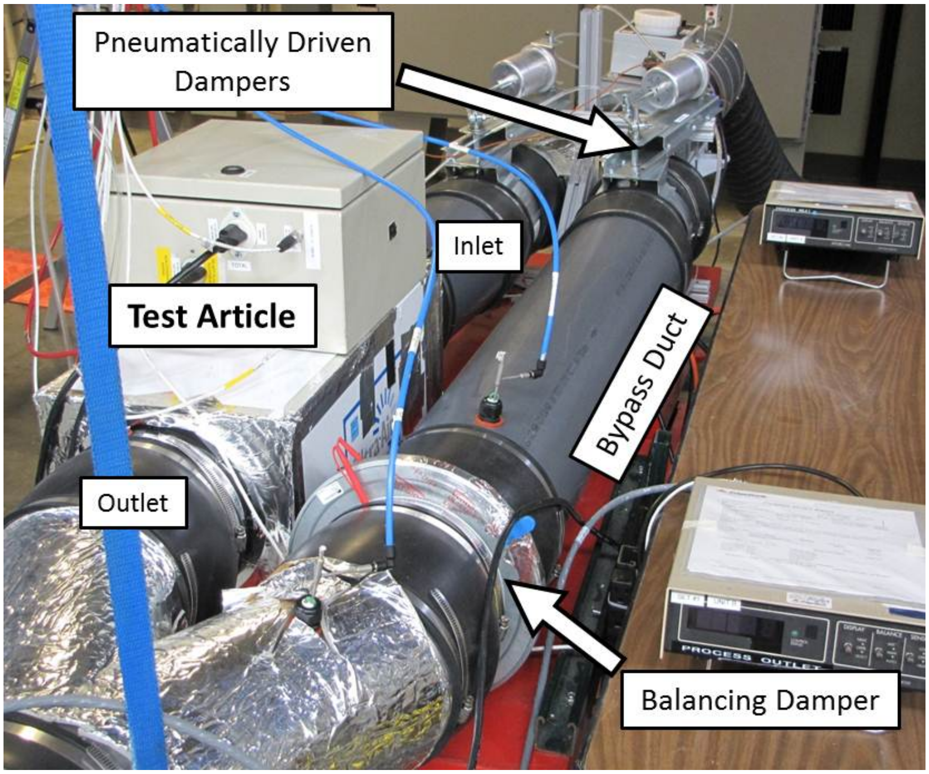

NREL/PIX 26755
Credit: Jon Winkler, NREL

Figure 3. Ultra-Aire 70H ducted dehumidifier test setup

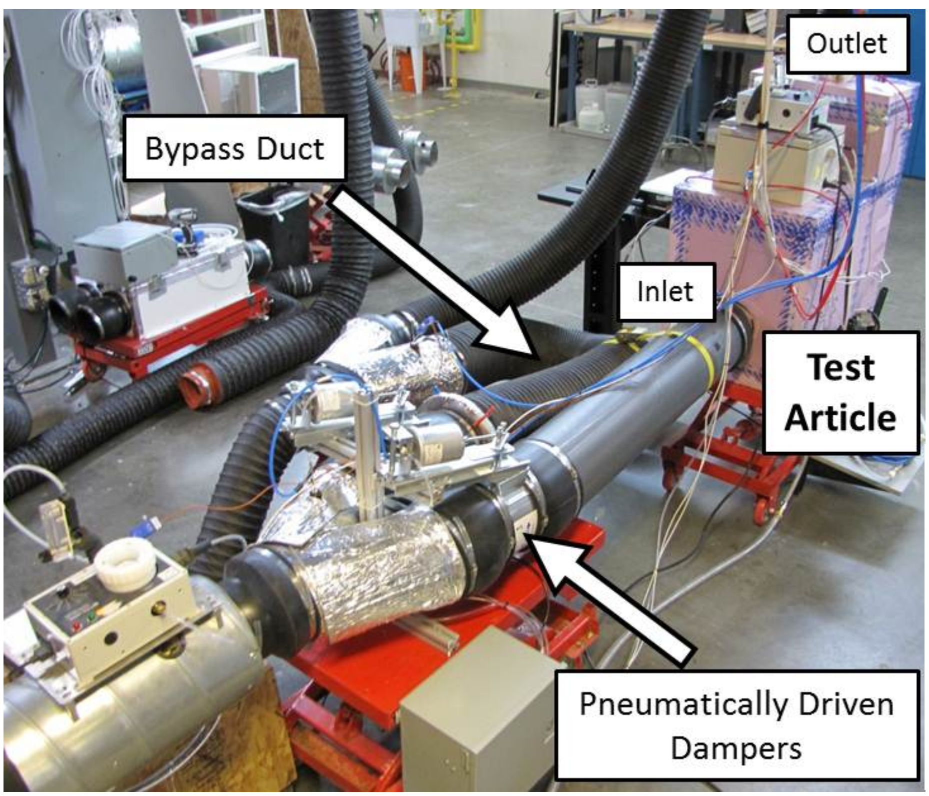

NREL/PIX 26758
Credit: Jon Winkler, NREL

Figure 4. GE standalone dehumidifier test setup

2.2 Test Matrix

The test matrix (Table 2) focused on testing each dehumidifier at different cycle rates and on-times at a fixed inlet DB temperature and RH. Thus, most tests occurred at test condition C1. However, three additional test conditions (C2–C4) were tested at a single cycling rate to determine the impact of the inlet condition on part load efficiency.

Table 2. Dehumidifier Cyclic Test Matrix

Test Condition	Inlet DB (°C)	Inlet DB (°F)	Inlet RH	RTF	CPH	τ_{on} (min)	τ_{off} (min)	N_{cyc}
C1	24.4	76	55%	20%	0.8	15	60	3
					1.2	10	40	3
					2	6	24	4
					3	4	16	6
					4	3	12	6
				50%	1	30	30	3
					3	10	10	4
					5	6	6	6
					10	3	3	8
				80%	1	48	12	3
					2	24	6	3
					4	12	3	5
					8	6	1.5	6
C2	24.4	76	60%	20%	2	6	24	4
C3	26.7	80	60%	20%	2	6	24	4
C4	20.0	68	65%	20%	2	6	24	4

For the purposes of this analysis, a cycle is defined as a period of dehumidifier operation followed by a period of idling. Thus,

$$\tau_{cyc} = \tau_{on} + \tau_{off} \tag{8}$$

The test matrix was developed using a CPH and runtime fraction (RTF), from which on- and off-times were calculated.

$$\tau_{on} = \frac{60}{CPH} \cdot RTF \tag{9}$$

$$\tau_{off} = \frac{60}{CPH} \cdot (1 - RTF) \tag{10}$$

The number of cycles run for each test was loosely determined by the on- and off-times. However, each on/off cycle was analyzed for consistency to reduce the need for a large number of cycles. ANSI/AHRI (2008) mandates a minimum of three complete on/off cycles for air conditioners and heat pumps. We followed that approach in the present work.

The test matrix listed in Table 2 was slightly modified for each dehumidifier. For example, the onboard controls of the two standalone units prevented the unit from running for less than 3 minutes. Thus, the test with a 1.5-minute off-time was not completed for these two units.

Fan operation coincided with compressor operation for the two ducted units. However, for the two standalone dehumidifiers, the fan operated for 3 additional minutes after the compressor shut off. Thus for the two standalone units, the times listed in Table 2 are the compressor on- and off-times. (This operational control strategy introduced significant latent degradation, especially for shorter runtimes [see Section 3].)

2.3 Analysis Method

The analysis method developed here for determining dehumidifier part load efficiency is analogous to the procedure used for air conditioners and heat pumps described in AHRI Standard 210/240 (ANSI/AHRI 2008) (see Section 1.2). Before each cyclic test, a steady-state test was conducted to determine steady-state capacity and efficiency used to calculate the part load degradation. Similar to air conditioners, the PLR was calculated using Equation 11.

$$PLR = \frac{M_{cyc}}{\dot{m}_{water,ss} \cdot \tau_{cyc}} \tag{11}$$

where,

$$M_{cyc} = \int^{\tau_{cyc}} \dot{m}_{air} \left(\omega_{in} - \omega_{out} \right) dt \tag{12}$$

The data analysis relied on air-side measurements to determine the part load moisture removal rate. Condensate was also measured and was within the uncertainty of the air-side calculated moisture removal. The two standalone dehumidifiers operated the fan 3 additional minutes after the compressor shut off, which added moisture to the dehumidifier airstream. The condensate measurement did not account for the moisture addition after the compressor shut off. Additionally, the evaporation rate of the retained condensate on the evaporator coil during the off-cycle was assumed to be quite slow compared to the off-time. Therefore, the added moisture due to evaporation of the retained condensate during the off-cycle was neglected.

Steady-state efficiency of a dehumidifier (η_{ss}) is often described in liters of water removed from the air per kilowatt-hour of electrical energy consumed. Efficiency for an on/off cycle was calculated in a similar fashion by integrating the water removed and total power use over the cycle.

$$\eta_{cyc} = \frac{M_{cyc}}{\int^{\tau_{cyc}} \dot{P}_{tot} \, dt} \tag{13}$$

M_{cyc} and η_{cyc} account for the latent degradation and additional fan energy that result from the control strategy of the two standalone units. (Section 4.2 will show that the poor part load performance caused by this control strategy can be attributed to latent degradation and not to additional fan energy, which was small compared to energy used during the entire on-cycle.)

The PLF and capacity degradation fraction (CDF) were calculated for each cyclic test.

$$PLF = \frac{\eta_{cyc}}{\eta_{ss}} \tag{14}$$

$$CDF = \frac{M_{cyc}}{\dot{m}_{ss} \cdot \tau_{cyc}} \tag{15}$$

Performance across all cycles was averaged to determine the part load performance for each test. Performance from cycle to cycle was highly repeatable for a given test; thus, there was little difference between selecting a single cycle (such as in AHRI Standard 210/240) and averaging across several cycles to calculate the part load performance.

3 Test Results and Analysis

Appendix B includes the complete set of cyclic experimental test data for all four test articles. Data tables in Appendix B include achieved test conditions, steady-state performance, degradation caused by cyclic operation, and overall uncertainty due to measurement error (calculated using procedures described by Taylor and Kyatt [1994]). As expected, the part load performance is dependent on the cycling characteristics. As shown in the data tables, the inlet air condition did not have a dramatic impact on the part load efficiency. Section 3.3 includes a table for the two standalone dehumidifiers comparing the total moisture removed during an on-cycle to the moisture reintroduced to the air after the compressor shuts off because of the 3 additional minutes of fan operation.

Steady-state performance of all four dehumidifiers compared well with previous steady-state testing (Winkler et al. 2011). Though the same inlet conditions were not previously tested, performance curves generated from previous steady-state testing predicted current steady-state performance to within 3%.

To develop PLF curves for use in EnergyPlus (DOE 2012), assumptions need to be made about dehumidistat operation in real homes. Data on installed dehumidifier cycling behavior are limited; however, data from two NREL-monitored houses in New Orleans, Louisiana, were used to estimate dehumidifier cycling behavior. The assumptions and procedure to develop the PLF curves are included in Section 4.

3.1 Time Series Results

Figure 5 and Figure 6 include time series data for the Ultra-Aire 70H ducted dehumidifier cycling at 2 CPH with a 20% RTF (24 minutes off, 6 minutes on) at test condition C1. Figure 5 includes inlet and outlet DB temperatures and RHs; Figure 6 plots moisture removal rate and total power consumption.

Steady-state data are collected during the first 8–10 minutes. The inlet DB and RH are held constant during the entire test. At the start of the cyclic test, the dehumidifier airstream damper closes and the dehumidifier fan and compressor are turned off.

The on/off cycling behavior is clearly seen in Figure 5 and Figure 6. The inrush current when the unit turns on is short and not always visible in the plot. The moisture removal rate reaches the steady-state value after a few minutes of operation. Because the fan and compressor shut off simultaneously, no moisture is added when the unit shuts down. We did not detect any added moisture addition at startup.

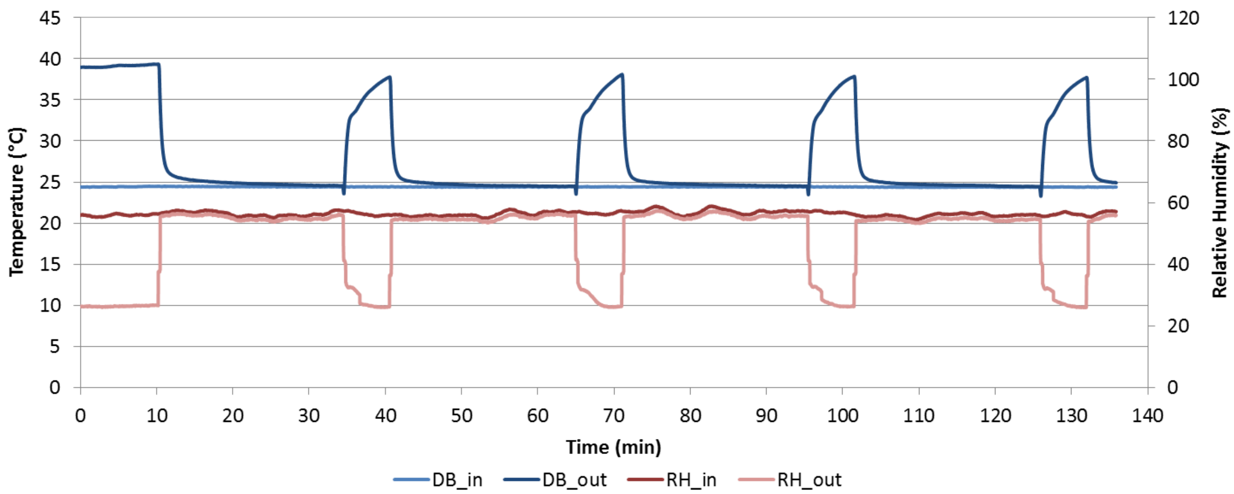

Figure 5. Time series plot showing ducted dehumidifier inlet and outlet conditions

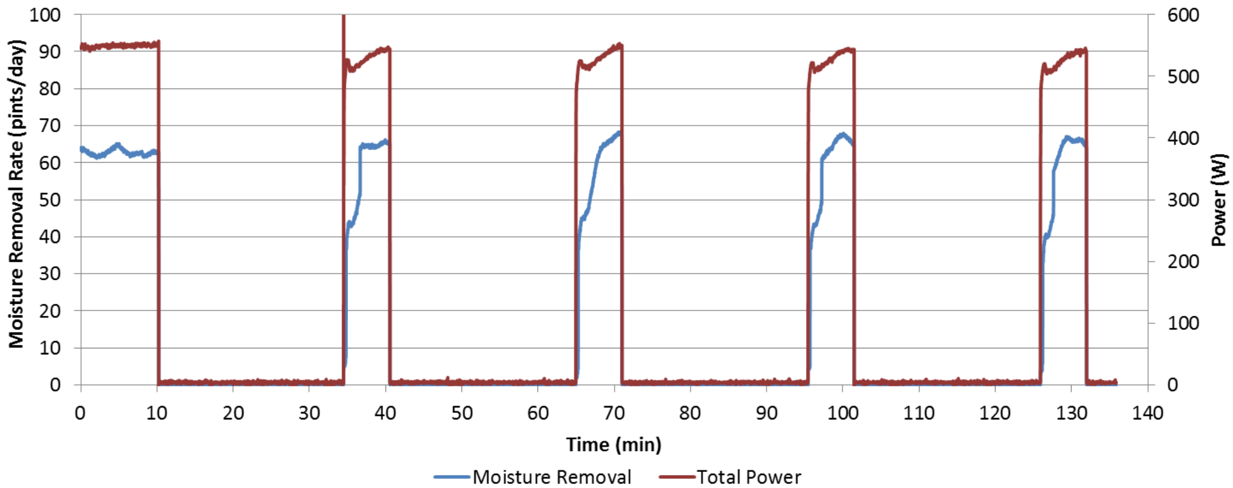

Figure 6. Time series plot showing ducted dehumidifier performance

Figure 7 and Figure 8 include time series data for the GE standalone dehumidifier cycling at 2 CPH with a 20% RTF (24 minutes off, 6 minutes on) at test condition C1. Figure 7 includes inlet and outlet DB temperatures and RHs; Figure 8 plots moisture removal rate and total power consumption. The experimental setup varied slightly from the ducted unit because of the standalone dehumidifier strategy; thus, the time series plots make sense only when the damper is open (and the dehumidifier fan is operating).

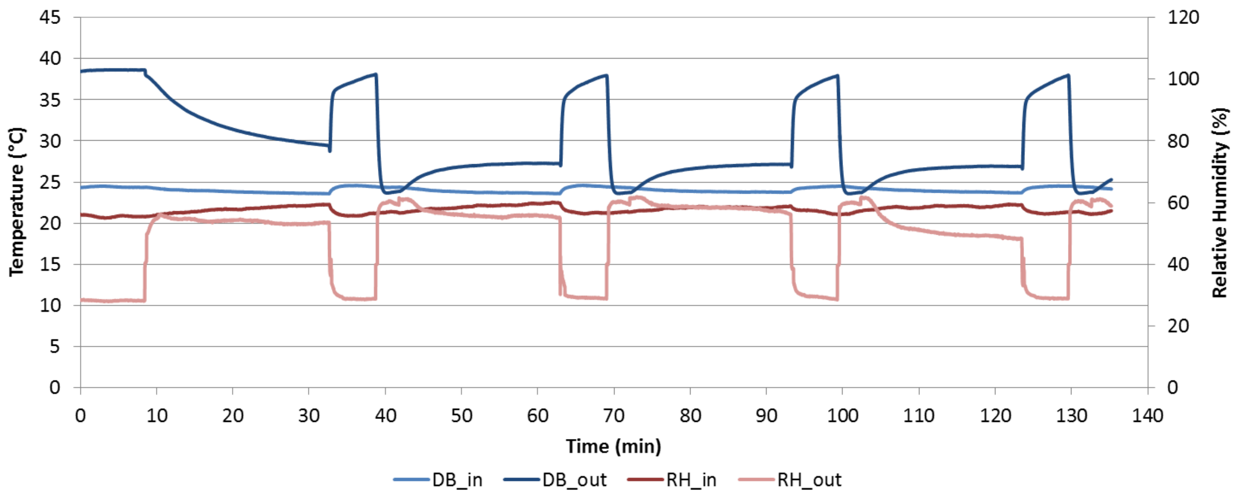

Figure 7. Time series plot showing standalone dehumidifier inlet and outlet conditions

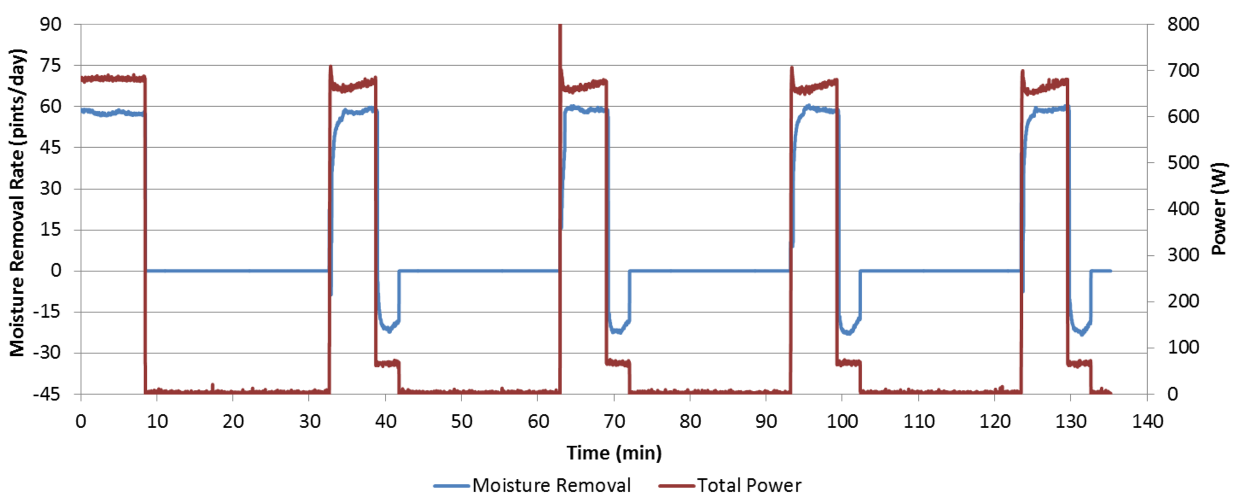

Figure 8. Time series plot showing standalone dehumidifier performance

Figure 8 clearly shows the control strategy used by the standalone unit. Following a period of dehumidification, the compressor shuts off but the fan continues to operate for 3 additional minutes. During this time the dehumidifier adds moisture to the airstream, which is evidenced by the negative moisture removal rate in Figure 8. (Note that the x-axis in Figure 8 intersects the left y-axis at –45 pints/day.) However, the startup response of the system performed very well. The unit reaches a steady-state capacity after 1–2 minutes of operation. Thus, the part load degradation presented in subsequent sections for this particular unit can be attributed mostly to the fan control strategy.

Additional time series plots have been omitted for brevity. However, all other cyclic tests were similar to those shown above and were individually examined to ensure consistency from cycle to cycle.

3.2 Part Load Test Results

Part-load performance data for each dehumidifier is included in Appendix B. This section explains trends in the part load performance for the Ultra-Aire 70H ducted dehumidifier and the GE 65 pint/day standalone unit. Part load performance plots for all four dehumidifiers are included in Appendix C. The plots in Appendix C are identical to plots in this section with the addition of error bars to display the overall measurement uncertainty. (Error bars are not included on the plots in this section to better display trends in the data.)

Figure 9 includes two plots depicting the part load performance of the Ultra-Aire 70H ducted dehumidifier. Figure 9a compares the PLR (calculated from time series data using Equation 11) to the CPH for different RTFs. Points in the plot were generated from the collected data and linear trend lines were added for visualization. As the CPH decreases (resulting in fewer on/off cycles) the PLR approaches the RTF. In building simulation tools, the PLR is determined by the space conditioning load (sensible or latent). However, the PLR of the equipment is clearly dependent on the cycling behavior and duty cycle.

Figure 9b plots the PLF as a function of PLR and RTF (calculated using Equation 14). Each point in the plot corresponds to a different CPH. (The corresponding CPH for each test can be determined from Figure 9a.) At lower RTFs, the PLF is very dependent on the CPH. As the CPH increases, the part load efficiency significantly decreases.

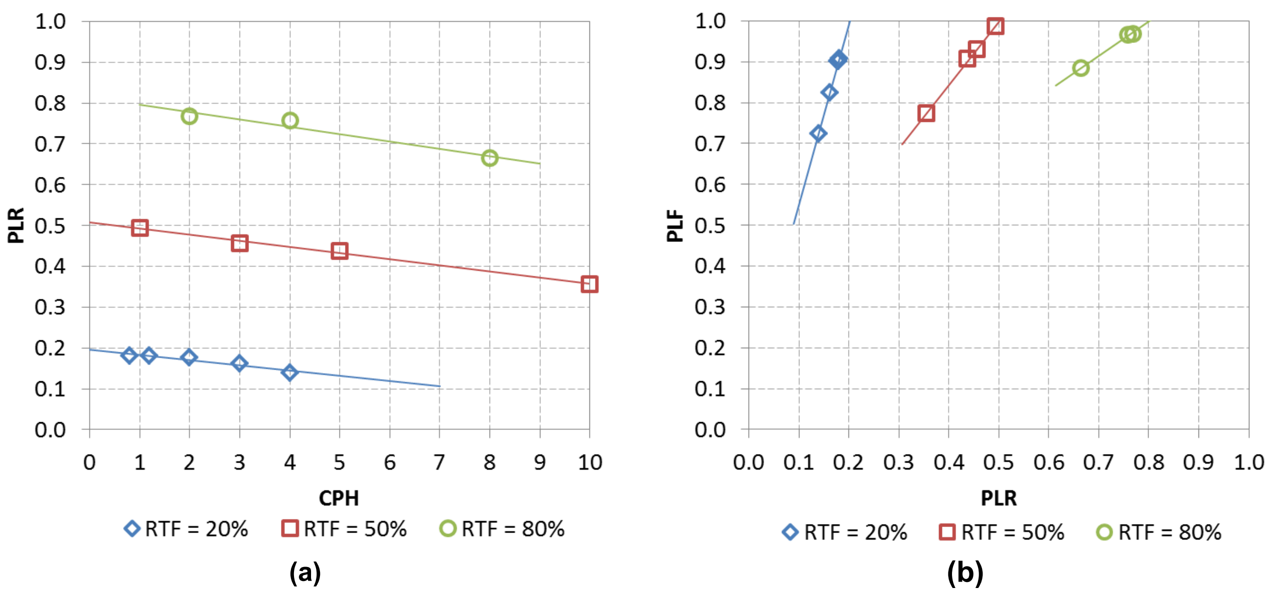

Figure 9. Part load performance plots for the Ultra-Aire 70H ducted dehumidifier

Figure 10 contains plots similar to Figure 9 for the standalone GE dehumidifier. The fan control strategy causes the part load performance to degrade at high cycling rates.

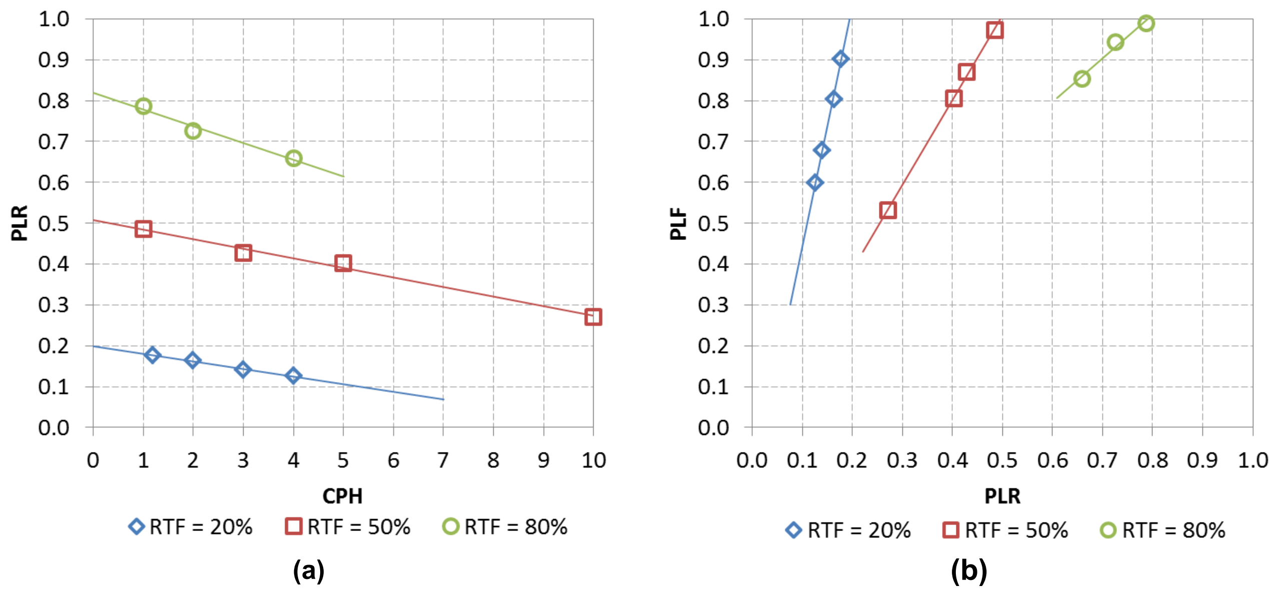

Figure 10. Part load performance plots for the GE standalone dehumidifier

3.3 Impacts of Standalone Dehumidifier Fan Control

Both standalone dehumidifiers operated the fan for 3 additional minutes after the compressor shut off. This control strategy greatly impacted the part load performance, particularly at high cycling rates. Table 3 emphasizes the impacts of the fan control strategy.

Table 3. Latent Degradation Impacts of Standalone Dehumidifier Fan Control

Cyclic Test Point					Moisture Removed/Added (per cycle)					
					GE Dehumidifier			Soleusaire Dehumidifier		
Test Condition	RTF (%)	CPH	t_{on} (min)	t_{off} (min)	Removed (cups)	Added (cups)	% Lost	Removed (cups)	Added (cups)	% Lost
C1	20%	1.2	10	40	0.82 ±0.05	0.09 ±0.02	10.5 ±2.5	0.62 ±0.03	0.07 ±0.01	11.2 ±2.0
		2	6	24	0.49 ±0.03	0.09 ±0.02	17.4 ±4.3	0.38 ±0.02	0.07 ±0.01	18.4 ±3.3
		3	4	16	0.33 ±0.02	0.09 ±0.02	27.3 ±6.4	0.24 ±0.01	0.07 ±0.01	30.0 ±5.0
		4	3	12	0.25 ±0.02	0.09 ±0.02	35.6 ±8.4	0.18 ±0.01	0.07 ±0.01	40.8 ±6.8
	50%	1	30	30	2.46 ±0.15	0.08 ±0.02	3.2 ±0.8	1.74 ±0.08	0.07 ±0.01	4.2 ±0.7
		3	10	10	0.81 ±0.05	0.08 ±0.02	9.9 ±2.5	0.61 ±0.03	0.07 ±0.01	11.0 ±2.0
		5	6	6	0.49 ±0.03	0.08 ±0.02	16.7 ±4.2	0.37 ±0.02	0.07 ±0.01	18.1 ±3.3
		10	3	3	0.23 ±0.01	0.09 ±0.02	38.5 ±8.9	0.18 ±0.01	0.08 ±0.01	42.1 ±7.0
	80%	1	48	12	3.94 ±0.24	0.08 ±0.02	2.0 ±0.5	2.78 ±0.13	0.07 ±0.01	2.6 ±0.4
		2	24	6	1.97 ±0.12	0.08 ±0.02	4.1 ±1.0	1.55 ±0.07	0.07 ±0.01	4.6 ±0.8
		4	12	3	0.96 ±0.06	0.09 ±0.02	9.0 ±2.1	0.74 ±0.03	0.07 ±0.01	9.7 ±1.7
C2	20%	2	6	24	0.58 ±0.03	0.07 ±0.02	12.2 ±3.7	0.40 ±0.02	0.07 ±0.01	16.2 ±3.2
C3		2	6	24	0.63 ±0.04	0.07 ±0.02	11.3 ±3.7	0.43 ±0.02	0.06 ±0.01	13.9 ±3.2
C4		2	6	24	0.60 ±0.03	0.03 ±0.02	5.8 ±3.0	0.34 ±0.01	0.06 ±0.01	16.4 ±3.0

Removed moisture is the total volume of moisture removed from the airstream while the compressor is on, and added moisture is the volume of moisture returned to the airstream while the fan runs for 3 minutes following the compressor. Percent lost is the ratio of added moisture to removed moisture.

The volume of moisture added after the compressor shut off was consistent from one test to the next and between both standalone units tested. The added moisture was a significant percentage of the removed moisture for short runtimes. Section 4.1 explains that short runtimes do occur with installed units. When runtimes range from 3–6 minutes, 17%–42% of the removed moisture is returned to the space because of the fan control strategy; meaning, 17%–42% of the energy spent to dehumidify the air was wasted.

Figure 11 graphically shows the latent degradation impacts as a function of the compressor runtime for test condition C1.

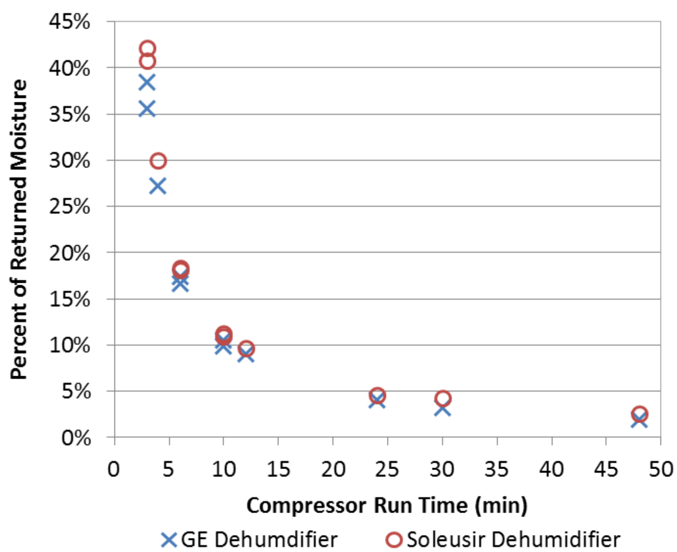

Figure 11. Latent degradation impacts of standalone dehumidifier fan control

The data tables in Appendix B also include the CDF for each test point. CDF values are considerably lower for cycle times with significant latent degradation.

4 Part Load Performance Curves

To account for part load efficiency degradation, the EnergyPlus DX dehumidifier model uses a PLF correlation to determine the additional runtime necessary to satisfy the predicted dehumidification load (DOE 2012). The model uses the following correlation to estimate the PLF.

$$PLF = a + b \cdot PLR + c \cdot PLR^2 \tag{16}$$

The data plotted in Figure 9b and Figure 10b cannot be fit to Equation 16 unless assumptions are made about dehumidifier cycling rate. Comprehensive datasets on the cycling behavior of installed residential dehumidification systems are not readily available; however, data from four NREL-monitored houses in New Orleans, Louisiana, were used to develop PLF curves.

4.1 Observed Dehumidifier Cycling Behavior

One-minute operational data collected from April through June 2013 on four whole-house dehumidifiers were analyzed to estimate dehumidifier cyclic behavior. Two of the homes contained ducted dehumidifiers and two included standalone dehumidifiers located in utility closets (with central fan integrated supply ventilation systems to provide fresh return air [Rudd 2003]). Similar cycling behavior was observed in both ducted dehumidifiers and both standalone dehumidifiers; however, the cycling behavior was quite different between the two dehumidifier types (likely because of installation practices). Both standalone dehumidifiers frequently short cycled; most runtimes lasted for less than 4 minutes.

Table 4 includes the dehumidifier cyclic information gathered from the field for the two dehumidifier types. The high CPH for the standalone dehumidifier is due to the frequent short cycling. The cause of the short cycling, whether installation practice, house characteristics, or characteristics particular to this product class, cannot be determined from the limited dataset.

Table 4. Dehumidifier Cyclic Field Data

RTF	CPH	
	Ducted	Standalone
0.2	0.9	6.0
0.5	2.3	8.0
0.8	1.9	4.4

Though there is a stark difference in the CPH in Table 4 between the two dehumidifier types, it is inappropriate to assume all ducted installations will see favorable cycling rates and standalone units will short cycle because of the limited number of homes in the dataset. However, the two sets of cycling information are useful to place limits on PLF correlations for the dehumidifiers experimentally tested in this study.

The development of the PLF correlations is presented in Section 4.2 and the designations have been changed to “Low CPH Dehumidifier” and “High CPH Dehumidifier” to shift focus from the dehumidifier types presented in Table 4 to the two sets of cycling rates.

4.2 Part Load Fraction Curve Fits

A similar approach to Parken et al. (1977) was used to develop PLF correlations for each test article. Correlations were developed for both sets of cycling assumptions listed in Table 4. For each set of cycling rates, a corresponding set of PLR and PLF values had to be calculated to develop PLF correlations.

The first step was to determine the PLR for the RTFs and CPHs included in Table 4. A linear regression on the PLR versus CPH data for each RTF (see Figure 9a and Figure 10a) was performed to provide PLR values at the assumed cycling rates. PLF linear regressions as a function of PLR and RTF (see Figure 9b and Figure 10b) were then used to determine the set of PLF values. The result was two sets of points represented by the black and gray dots in Figure 12. (Figure 12 is Figure 9b with the addition of PLF versus PLR curves.) A PLR of 1.0 results in continuous operation; thus, the PLF must equal 1.0 at this point.

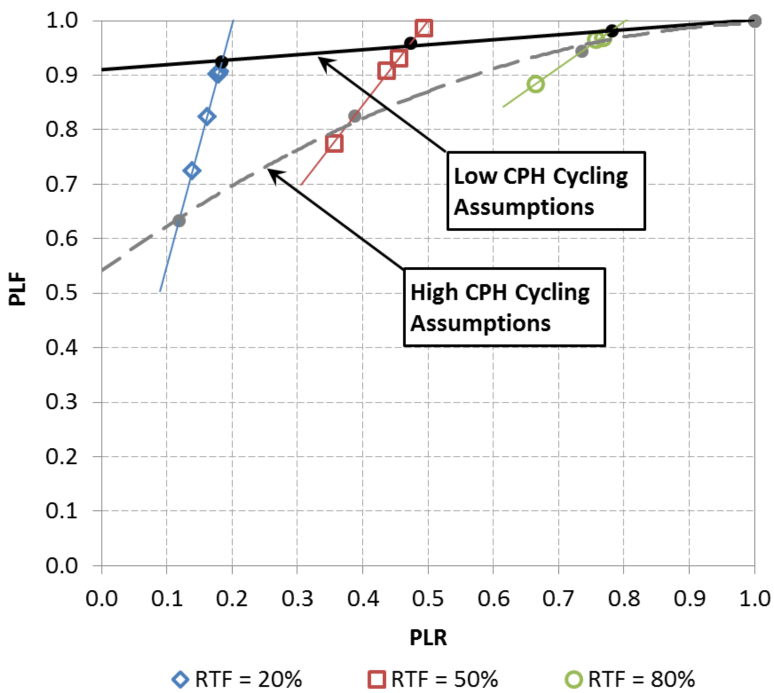

Figure 12. PLF performance curves for the Ultra-Aire 70H ducted dehumidifier

The Ultra-Aire 70H ducted dehumidifier PLF versus PLR curves for the two assumed cycling rates are shown in Figure 12. As expected, the cycling rate has a significant impact on the part load efficiency. For example, at a PLR of 0.2 and a low cycling rate the PLF is greater than 90%. However at a high cycling rate, the PLF falls to 70%.

The GE standalone dehumidifier PLF versus PLR curves for the two assumed cycling rates are shown in Figure 13. At a low cycling rate, the PLF curves for GE standalone dehumidifier and Ultra-Aire 70H ducted dehumidifier are quite similar. Both are efficient under part load operation. However, with a high cycling rate, the performance of the standalone unit significantly decreases compared to the ducted unit. With a high cycling rate and at a PLR of 0.2, the standalone unit has a PLF of 0.5 compared to 0.7 for the ducted unit. Thus, at a high cycling rate and a PLR of 0.2, the standalone unit is operating at an efficiency of 50% compared to the steady-state efficiency.

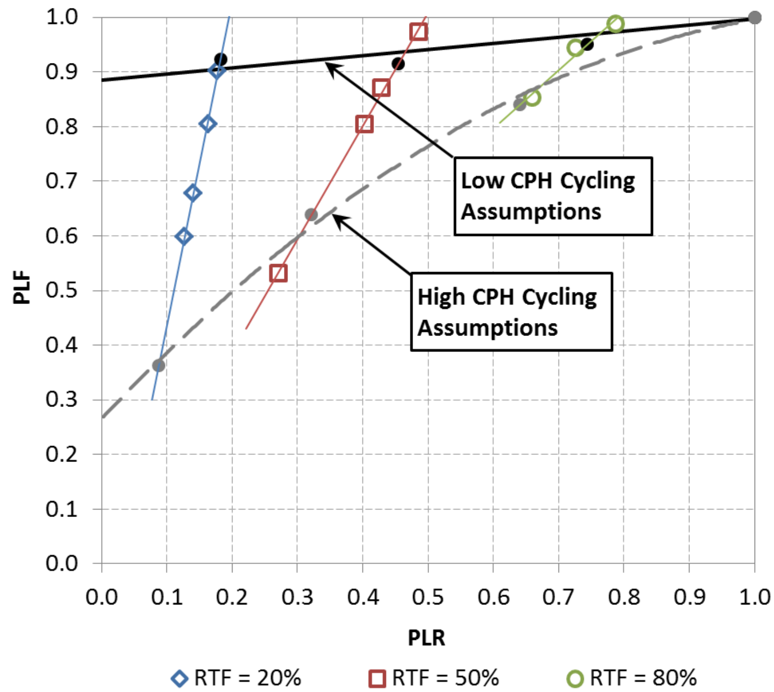

Figure 13. PLF performance curves for the GE standalone dehumidifier

PLF performance curves for all four dehumidifiers are included in Appendix D. The part load efficiency of the Ultra-Aire XT150H was lower than that of its ducted counterpart, the 70H. This was likely attributable to larger heat exchangers, additional refrigerant charge, and the added air-to-air wraparound heat exchanger. The fan control strategy of the standalone units was the main driver in the part load performance. Thus, both standalone units had similar part load performance.

4.3 Part Load Fraction Curve Coefficients

The solid black and dashed gray curves in Figure 12 and Figure 13 are the PLF performance curves for the two test articles. Because only four points were used to develop the PLF performance curve, the cubic polynomial expressed in Equation 16 cannot be used. Thus, quadratic and linear relationships were used. Quadratic curve fits best represented the high CPH PLF curves, whereas linear relationships worked best for the low CPH PLF curves. Table 5 includes the coefficients for Equation 16 for each of the four test articles under both the low and high CPH assumptions.

Table 5. Dehumidifier PLF Curve Coefficients

Dehumidifier	CPH	PLF Curve Coefficients		
		a	***b***	***c***
Ultra Aire XT150H	Low	0.8078	0.1880	0
	High	0.2196	1.4473	–0.6776
Ultra Aire 70H	Low	0.9103	0.0913	0
	High	0.5412	0.8624	–0.4080
GE ADER65LP	Low	0.8843	0.1126	0
	High	0.2655	1.2666	–0.5369
Soleusair SG-DEH-45-1	Low	0.8908	0.1069	0
	High	0.2037	1.5161	–0.7279

5 Conclusions

This report describes part load performance testing of four residential DX dehumidifiers to enable whole-building integration analysis. Unlike residential air-conditioning and heat pumping equipment, part load testing is not mandated by the dehumidifier test standard. Thus, part load performance of residential dehumidifiers has not, to our knowledge, previously been measured. All testing was conducted at NREL's Advanced HVAC Systems Laboratory.

HVAC equipment rarely operates at steady state, and characterizing dehumidifier performance under cycling operation is an important step in estimating residential dehumidifier energy use in real-world applications. The part load performance testing described in this report complements a previous study presented in Winkler et al. (2011) investigating the steady-state performance of residential dehumidifiers under a variety of indoor conditions. The two reports combine to provide a comprehensive dataset to accurately model residential dehumidifiers under a variety of operating conditions and part load scenarios.

Residential DX dehumidifiers fall into two categories—ducted and standalone. Two dehumidifiers of each type were tested under 13 cycling scenarios. Field data from two NREL-monitored houses were used to develop two PLF performance curves for each test article. The limited field data indicate that short cycling does occur. Cycling rates have a significant impact on the part load efficiency, and measures should be taken to prevent short cycling. At low cycling rates, the part load efficiency was typically 85% or higher. However, the performance greatly degraded at high cycling rates and the part load efficiency fell to less than half the steady-state value. Thus, designing the dehumidistat to prevent short cycling is critical to minimizing cyclic losses.

Both standalone dehumidifiers ran the fan for 3 minutes longer than the compressor, which resulted in significant latent degradation. The reasoning behind this control strategy is not evident, but could be intended to prevent short cycling caused by the RH sensor being mounted on the inlet side of the evaporator coil. Testing indicated that 17%–42% of the moisture removed by the dehumidifier was returned to the space when compressor runtime was 3–6 minutes. Thus with short runtimes, a significant portion of the energy used to dehumidify the air is wasted. Table 6 summarizes two control strategy improvements that would significantly improve dehumidifier part load performance.

Table 6. Summary of Potential Control Strategy Improvements

Recommended Control Modification	Potential Outcome	Potential Part Load Efficiency Improvement
Eliminate Extended Fan Operation	• Significantly reduce latent degradation • Reduce dehumidifier runtime by reducing moisture addition following compressor operation	Up to 20% (at high cycling rates)
Increase Dehumidistat RH Dead Band	• Prevent dehumidifier from short cycling caused by inadequate air mixing • Encourage longer dehumidifier runtimes	Up to 30%–60% (depending on fan control strategy)

References

ANSI/AHAM. (2008). Association of Home Appliance Manufacturers – Dehumidifiers. ANSI/AHAM DH-1-2008. Washington, DC: Association of Home Appliance Manufacturers.

ANSI/AHRI. (2008). Performance Rating of Unitary Air-Conditioning and Air Source Heat Pump Equipment. ANSI/AHRI Standard 210/240. Arlington, VA: Air-Conditioning, Heating, and Refrigeration Institute.

Cutler, D.; Winkler, J.; Kruis, N.; Christensen, C.; Brandemuehl, M. (2013). *Improved Modeling of Residential Air Conditioners and Heat Pumps for Energy Calculations*. NREL/TP-5500-56354. Golden, CO: National Renewable Energy Laboratory.

DOE. (2012). EnergyPlus Engineering Reference. Washington, DC: U.S. Department of Energy.

Fang, X.; Winkler, J.; Christensen, D. (2011). "Using EnergyPlus to Perform Dehumidification Analysis on Building America Homes." *HVAC&R Research* 17(3):268–283.

Henderson, H.; Huang, Y.J.; Parker, D. (1999). *Residential Equipment Part Load Curves for use in DOE-2*. LBNL-42175. Berkeley, CA: Lawrence Berkeley National Laboratory.

Parken, W.; Beausoliel, R.; Kelley, G. (1977). "Factors Affecting the Performance of a Residential Air-to-Air Heat Pump." *ASHRAE Transactions* 83(1):839–849

Rudd, A. (2003). *Central Fan Integrated Supply Ventilation – The Basics*. Research Report – 0304. Somerville, MA: Building Science Corporation.

Taylor, B.N.; Kuyatt, C.E. (1994). *Guidelines for Evaluating and Experssing the Uncertainty of NIST Measurement Results*. NIST Technical Note 1297. Gaithersburg, MD: National Institute of Standards and Technology.

Winkler, J.; Christensen, D.; Tomerlin, J. (2011). *Laboratory Test Report for Six ENERGY STAR Dehumidifiers*. NREL/TP-5500-52791. Golden, CO: National Renewable Energy Laboratory.

Appendix A: Photographs of Experimental Setup

Figure 14 shows the test setup for the Ultra-Aire XT150H ducted dehumidifier. The inlet and outlet dew point hygrometers are shown in the lower left corner of the photograph. The hygrometers did not need to be placed exactly at the unit's inlet and outlet because of the high airflow rate.

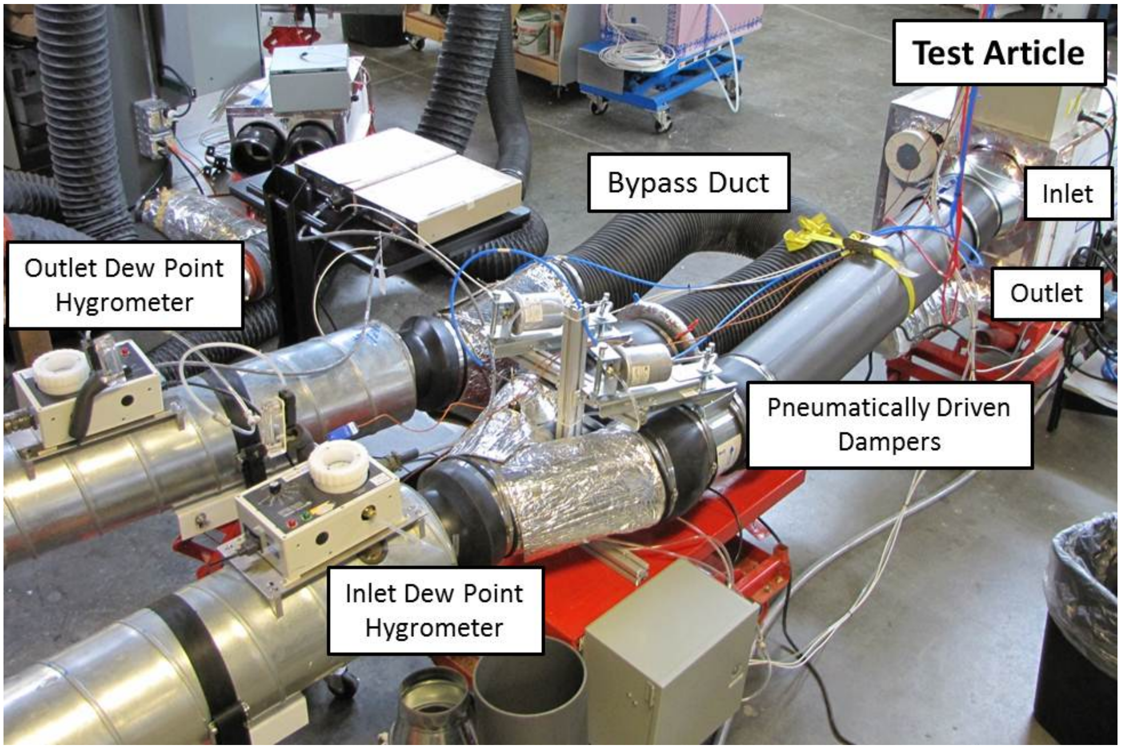

NREL/PIX 26756
Credit: Jon Winkler, NREL

Figure 14. Ultra-Aire XT150H ducted dehumidifier test setup

Figure 15 shows another photograph of the Ultra-Aire 70H test setup (similar to Figure 3). Air flows from left to right. The box on top of the dehumidifier includes two power meters used to individually measure the fan and total unit power. The outlet dew point hygrometer (upper right) is located in close proximity to the outlet because of the lower airflow rate. The PD, fast-acting sealing dampers direct laboratory conditioned air through the unit or through the bypass duct, depending on the unit's on/off status. The inset image shows a zoomed in picture of the PD dampers.

NREL/PIX 26754 (top), 26753 (bottom)
Credit: Jon Winkler, NREL

Figure 15. Ultra-Aire 70H ducted dehumidifier test setup (top) with PD damper system (bottom)

Figure 16 includes another photo of the GE standalone dehumidifier test setup (similar to Figure 4). Photographs of the Soleusair standalone dehumidifier are not shown, because the test setup was identical for both standalone dehumidifiers.

NREL/PIX 26757
Credit: Jon Winkler, NREL

Figure 16. GE standalone dehumidifier test setup

Appendix B: Summary of Measured and Calculated Test Data

Table 7. Cyclic Experimental Test Data for the Ultra-Aire XT150H Ducted Dehumidifier

Cyclic Test Point					Steady State Results (prior to cyclic operation)					Cyclic Test						
Test Condition	**RTF (%)**	**CPH**	**t_{on} (min)**	**t_{off} (min)**	**DB_{in} (°C)**	**RH_{in} (%)**	**Capacity (pints/day)**	**η_{ss} (L/kWh)**	**Total Power (W)**	**DB_{in} (°C)**	**RH_{in} (%)**	**Capacity[1] (pints/day)**	**η_{ss}[2] (L/kWh)**	**PLR**	**PLF**	**CDF**
C1	**20%**	**0.8**	15	60	24.4	55.1	121.5 ±6.0	3.2 ±0.2	741	24.4	55.1	106.1 ±6.0	2.8 ±0.2	0.17 ±0.01	0.87 ±0.06	0.87 ±0.06
		1.2	10	40	24.2	56.1	123.2 ±6.1	3.3 ±0.2	738	24.2	55.1	98.2 ±6.1	2.6 ±0.2	0.16 ±0.01	0.80 ±0.06	0.80 ±0.06
		2	6	24	24.4	56.5	125.2 ±6.2	3.3 ±0.2	743	24.4	55.7	88.5 ±6.2	2.4 ±0.2	0.14 ±0.01	0.72 ±0.06	0.71 ±0.06
		3	4	16	24.4	54.8	120.0 ±6.0	3.2 ±0.2	741	24.4	55.9	75.4 ±6.3	2.0 ±0.2	0.13 ±0.01	0.64 ±0.06	0.63 ±0.06
		4	3	12	24.4	56.1	122.4 ±6.1	3.2 ±0.2	742	24.3	54.6	57.6 ±6.2	1.6 ±0.2	0.09 ±0.01	0.49 ±0.06	0.47 ±0.06
	50%	**1**	30	30	24.4	53.5	115.0 ±5.8	3.1 ±0.2	736	24.3	53.8	107.5 ±5.9	2.9 ±0.2	0.47 ±0.03	0.94 ±0.07	0.94 ±0.07
		3	10	10	24.4	54.2	117.4 ±5.9	3.1 ±0.2	739	24.3	54.5	98.0 ±6.0	2.6 ±0.2	0.42 ±0.03	0.85 ±0.07	0.83 ±0.06
		5	6	6	24.4	54.1	115.2 ±5.9	3.1 ±0.2	738	24.4	55.0	86.5 ±6.1	2.4 ±0.2	0.37 ±0.03	0.76 ±0.07	0.75 ±0.06
	80%	**1**	48	12	24.5	54.7	118.7 ±6.0	3.2 ±0.2	740	24.4	55.6	115.7 ±6.0	3.1 ±0.2	0.78 ±0.05	0.97 ±0.07	0.97 ±0.07
		2	24	6	24.4	53.5	113.3 ±5.9	3.0 ±0.2	736	24.4	54.3	107.4 ±5.9	2.9 ±0.2	0.75 ±0.06	0.95 ±0.07	0.95 ±0.07
		4	12	3	24.4	55.7	120.2 ±6.1	3.2 ±0.2	743	24.4	55.0	101.9 ±6.0	2.7 ±0.2	0.67 ±0.05	0.86 ±0.07	0.85 ±0.06
C2	**20%**	**2**	6	24	24.5	59.7	132.4 ±6.5	3.5 ±0.2	753	24.5	59.2	96.6 ±6.6	2.6 ±0.2	0.15 ±0.01	0.74 ±0.06	0.73 ±0.06
C3		**2**	6	24	26.6	60.7	147.0 ±7.4	3.7 ±0.2	793	26.5	61.2	110.8 ±7.5	2.8 ±0.2	0.15 ±0.01	0.77 ±0.06	0.75 ±0.06
C4		**2**	6	24	20.2	63.2	116.4 ±5.4	3.3 ±0.2	692	20.4	63.4	86.4 ±5.5	2.5 ±0.2	0.15 ±0.01	0.75 ±0.06	0.74 ±0.06

[1] Average capacity calculated while the dehumidifier was operating
[2] Average efficiency calculated during the entire cycle

Table 8. Cyclic Experimental Test Data for the Ultra-Aire 70H Ducted Dehumidifier

Cyclic Test Point					Steady State Results (prior to cyclic operation)					Cyclic Test						
Test Condition	RTF (%)	CPH	t_{on} (min)	t_{off} (min)	DB_{in} (°C)	RH_{in} (%)	Capacity (pints/day)	η_{ss} (L/kWh)	Total Power (W)	DB_{in} (°C)	RH_{in} (%)	Capacity[1] (pints/day)	η_{ss}[2] (L/kWh)	PLR	PLF	CDF
C1	20%	**0.8**	15	60	24.4	56.0	61.9 ±3.1	2.2 ±0.1	546	24.4	54.0	55.8 ±3.0	2.0 ±0.1	0.18 ±0.01	0.90 ±0.06	0.90 ±0.06
		1.2	10	40	24.2	56.9	63.0 ±3.1	2.3 ±0.1	546	24.4	56.2	57.2 ±3.1	2.1 ±0.1	0.18 ±0.01	0.91 ±0.06	0.91 ±0.06
		2	6	24	24.4	55.9	62.8 ±3.1	2.3 ±0.1	549	24.4	56.5	56.0 ±3.1	2.0 ±0.1	0.18 ±0.01	0.90 ±0.07	0.89 ±0.06
		3	4	16	24.4	55.4	60.2 ±3.0	2.2 ±0.1	544	24.5	55.9	49.0 ±3.1	1.8 ±0.1	0.16 ±0.01	0.82 ±0.07	0.81 ±0.06
		4	3	12	24.5	55.9	61.9 ±3.1	2.2 ±0.1	551	24.5	56.0	43.5 ±3.2	1.6 ±0.1	0.14 ±0.01	0.72 ±0.06	0.70 ±0.06
	50%	**1**	30	30	24.4	56.6	62.8 ±3.1	2.3 ±0.1	546	24.4	57.3	62.3 ±3.1	2.2 ±0.1	0.49 ±0.03	0.99 ±0.07	0.99 ±0.07
		3	10	10	24.4	55.3	60.8 ±3.0	2.2 ±0.1	542	24.4	54.7	56.4 ±3.0	2.1 ±0.1	0.46 ±0.03	0.93 ±0.07	0.93 ±0.07
		5	6	6	24.4	55.6	61.2 ±3.1	2.2 ±0.1	550	24.5	55.5	54.9 ±3.1	2.0 ±0.1	0.44 ±0.03	0.91 ±0.07	0.90 ±0.07
		10	3	3	24.3	57.1	63.1 ±3.1	2.3 ±0.1	548	24.4	57.5	47.7 ±3.2	1.8 ±0.1	0.36 ±0.03	0.77 ±0.06	0.76 ±0.06
	80%	**2**	24	6	24.3	56.6	63.0 ±3.1	2.3 ±0.1	543	24.4	56.0	61.2 ±3.1	2.2 ±0.1	0.77 ±0.05	0.97 ±0.07	0.97 ±0.07
		4	12	3	24.2	56.5	60.7 ±3.1	2.2 ±0.1	542	24.4	56.3	58.8 ±3.1	2.1 ±0.1	0.76 ±0.05	0.97 ±0.07	0.97 ±0.07
		8	6	1.5	24.4	55.7	61.0 ±3.1	2.2 ±0.1	542	24.3	54.3	53.2 ±3.0	2.0 ±0.1	0.66 ±0.05	0.88 ±0.07	0.87 ±0.06
C2	20%	**2**	6	24	24.4	59.8	67.9 ±3.3	2.4 ±0.1	555	24.4	59.7	59.0 ±3.3	2.1 ±0.1	0.17 ±0.01	0.88 ±0.06	0.87 ±0.06
C3		**2**	6	24	26.8	59.8	79.3 ±3.7	2.7 ±0.1	588	26.7	59.9	68.4 ±3.7	2.3 ±0.1	0.17 ±0.01	0.88 ±0.06	0.86 ±0.06
C4		**2**	6	24	20.0	66.1	62.2 ±2.8	2.4 ±0.1	509	20.0	66.3	54.0 ±2.8	2.1 ±0.1	0.17 ±0.01	0.86 ±0.06	0.87 ±0.06

[1] Mean capacity calculated while the dehumidifier was operating
[2] Mean efficiency calculated during the entire cycle

Table 9. Cyclic Experimental Test Data for the GE ADER65LP Standalone Dehumidifier

Cyclic Test Point					Steady State Results (prior to cyclic operation)					Cyclic Test						
Test Condition	**RTF (%)**	**CPH**	**t_{on} (min)**	**t_{off} (min)**	**DB_{in} (°C)**	**RH_{in} (%)**	**Capacity (pints/day)**	**η_{ss} (L/kWh)**	**Total Power (W)**	**DB_{in} (°C)**	**RH_{in} (%)**	**Capacity[1] (pints/day)**	**η_{ss}[2] (L/kWh)**	**PLR**	**PLF**	**CDF**
C1	**20%**	**1.2**	10	40	24.4	55.1	57.1 ±3.6	1.7 ±0.1	679	24.3	56.0	40.1 ±3.7	1.5 ±0.1	0.18 ±0.02	0.90 ±0.10	0.70 ±0.08
		2	6	24	24.4	55.5	57.7 ±3.6	1.7 ±0.1	679	24.4	56.8	32.1 ±3.8	1.3 ±0.2	0.16 ±0.01	0.80 ±0.11	0.56 ±0.07
		3	4	16	24.4	56.4	58.9 ±3.6	1.7 ±0.1	683	24.3	56.0	24.0 ±3.8	1.2 ±0.2	0.14 ±0.01	0.68 ±0.11	0.41 ±0.07
		4	3	12	24.4	55.8	58.2 ±3.6	1.7 ±0.1	675	24.4	56.2	18.9 ±3.8	1.0 ±0.2	0.13 ±0.01	0.60 ±0.12	0.32 ±0.07
	50%	**1**	30	30	24.4	55.0	57.6 ±3.5	1.7 ±0.1	675	24.4	56.0	51.7 ±3.6	1.6 ±0.1	0.49 ±0.04	0.97 ±0.09	0.90 ±0.08
		3	10	10	24.4	56.2	59.1 ±3.6	1.7 ±0.1	682	24.4	55.8	40.2 ±3.7	1.5 ±0.1	0.43 ±0.04	0.87 ±0.09	0.68 ±0.07
		5	6	6	24.4	55.4	57.7 ±3.6	1.7 ±0.1	679	24.4	55.9	32.2 ±3.7	1.3 ±0.2	0.40 ±0.04	0.80 ±0.10	0.56 ±0.07
		10	3	3	24.4	55.5	58.5 ±3.6	1.7 ±0.1	677	24.4	55.4	17.1 ±3.8	0.9 ±0.2	0.27 ±0.03	0.53 ±0.12	0.29 ±0.07
	80%	**1**	48	12	24.4	55.0	57.7 ±3.5	1.7 ±0.1	677	24.4	55.8	54.4 ±3.6	1.7 ±0.1	0.79 ±0.07	0.99 ±0.09	0.94 ±0.08
		2	24	6	24.4	55.8	59.0 ±3.5	1.7 ±0.1	679	24.4	55.8	50.1 ±3.6	1.6 ±0.1	0.73 ±0.06	0.94 ±0.09	0.85 ±0.08
		4	12	3	24.4	56.5	60.0 ±3.7	1.7 ±0.1	681	24.4	54.9	41.5 ±3.6	1.5 ±0.1	0.66 ±0.06	0.85 ±0.09	0.69 ±0.07
C2	**20%**	**2**	6	24	24.4	61.2	67.1 ±3.9	1.9 ±0.1	692	24.6	60.5	39.9 ±4.0	1.7 ±0.2	0.17 ±0.01	0.86 ±0.10	0.59 ±0.07
C3		**2**	6	24	26.8	60.0	70.5 ±4.4	1.9 ±0.1	735	26.7	60.0	43.8 ±4.5	1.7 ±0.2	0.18 ±0.01	0.92 ±0.11	0.62 ±0.07
C4		**2**	6	24	19.6	72.0	66.5 ±3.5	2.1 ±0.1	638	19.5	74.4	44.2 ±3.7	2.0 ±0.2	0.20 ±0.01	0.96 ±0.09	0.66 ±0.06

[1] Mean capacity calculated while the dehumidifier was operating
[2] Mean efficiency calculated during the entire cycle

Table 10. Cyclic Experimental Test Data for the Soleusair SG-DEH-45-1 Standalone Dehumidifier

Cyclic Test Point					Steady State Results (prior to cyclic operation)					Cyclic Test						
Test Condition	RTF (%)	CPH	t_{on} (min)	t_{off} (min)	DB_{in} (°C)	RH_{in} (%)	Capacity (pints/day)	η_{ss} (L/kWh)	Total Power (W)	DB_{in} (°C)	RH_{in} (%)	Capacity[1] (pints/day)	η_{ss}[2] (L/kWh)	PLR	PLF	CDF
C1	20%	1.2	10	40	24.3	56.4	42.6 ±1.9	1.6 ±0.1	539	24.4	58.9	30.0 ±2.1	1.4 ±0.1	0.18 ±0.01	0.90 ±0.07	0.70 ±0.06
		2	6	24	25.1	57.8	44.8 ±2.1	1.6 ±0.1	554	24.9	58.3	24.2 ±2.2	1.3 ±0.1	0.16 ±0.01	0.81 ±0.08	0.54 ±0.05
		3	4	16	24.3	57.1	43.0 ±2.0	1.6 ±0.1	537	24.1	57.5	16.9 ±2.1	1.1 ±0.1	0.14 ±0.01	0.67 ±0.09	0.39 ±0.05
		4	3	12	24.3	57.4	43.3 ±2.0	1.6 ±0.1	537	24.5	57.0	12.4 ±2.1	.9 ±0.1	0.11 ±0.01	0.54 ±0.09	0.29 ±0.05
	50%	1	30	30	24.3	54.6	40.6 ±1.9	1.5 ±0.1	536	24.4	55.1	36.1 ±1.9	1.4 ±0.1	0.48 ±0.03	0.97 ±0.07	0.89 ±0.06
		3	10	10	24.3	57.5	43.8 ±2.0	1.6 ±0.1	538	24.6	57.1	29.9 ±2.1	1.4 ±0.1	0.43 ±0.03	0.87 ±0.07	0.68 ±0.06
		5	6	6	24.4	58.5	44.9 ±2.1	1.6 ±0.1	547	24.4	58.8	24.2 ±2.1	1.3 ±0.1	0.39 ±0.03	0.79 ±0.08	0.54 ±0.05
		10	3	3	24.4	57.3	43.6 ±2.0	1.6 ±0.1	543	24.5	57.9	12.2 ±2.2	0.8 ±0.2	0.26 ±0.03	0.53 ±0.10	0.28 ±0.05
	80%	1	48	12	24.4	55.4	41.9 ±2.0	1.5 ±0.1	539	24.3	55.8	38.2 ±2.0	1.5 ±0.1	0.76 ±0.05	0.96 ±0.07	0.91 ±0.06
		2	24	6	24.6	59.2	45.1 ±2.1	1.6 ±0.1	549	25.0	60.2	39.3 ±2.2	1.6 ±0.1	0.76 ±0.05	0.97 ±0.07	0.87 ±0.06
		4	12	3	24.5	58.9	45.2 ±2.1	1.6 ±0.1	546	24.4	58.3	31.8 ±2.1	1.4 ±0.1	0.67 ±0.04	0.87 ±0.07	0.70 ±0.06
C2	20%	2	6	24	24.9	62.5	49.4 ±2.3	1.8 ±0.1	556	25.0	61.0	26.6 ±2.3	1.4 ±0.1	0.16 ±0.01	0.80 ±0.08	0.54 ±0.05
C3		2	6	24	26.9	59.7	50.4 ±2.4	1.7 ±0.1	577	26.6	61.2	28.8 ±2.5	1.5 ±0.1	0.17 ±0.01	0.86 ±0.08	0.57 ±0.06
C4		2	6	24	20.1	64.1	40.6 ±1.7	1.6 ±0.1	501	20.0	65.5	22.6 ±1.8	1.3 ±0.1	0.16 ±0.01	0.81 ±0.07	0.56 ±0.05

[1] Mean capacity calculated while the dehumidifier was operating
[2] Mean efficiency calculated during the entire cycle

Appendix C: Part Load Performance Plots

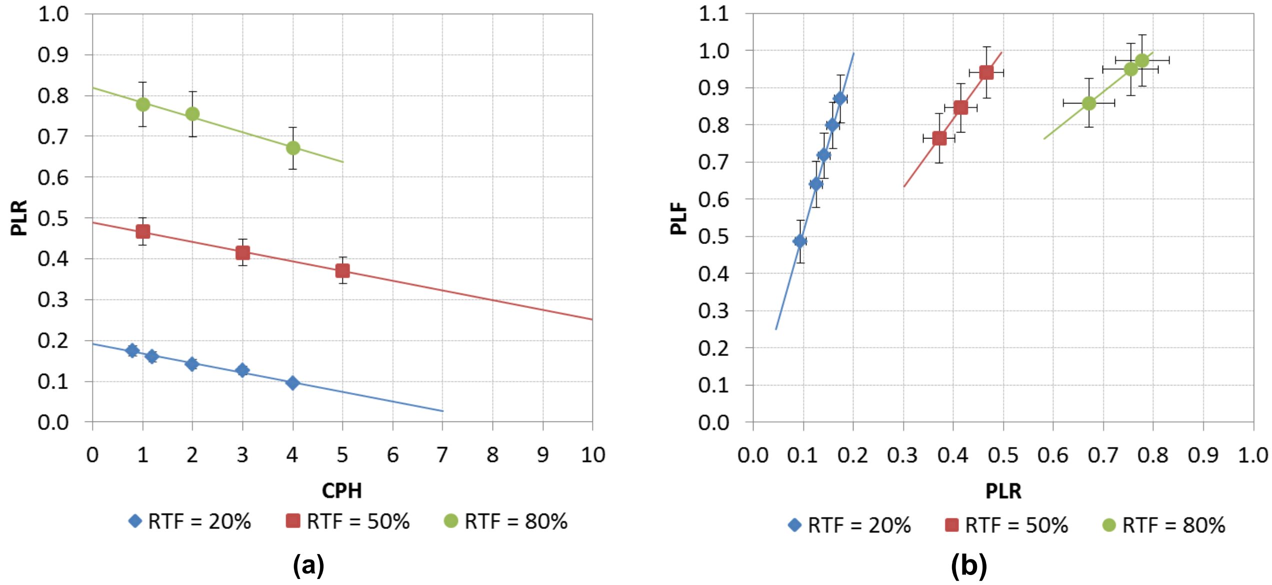

Figure 17. Part load performance plots for the Ultra-Aire XT150H ducted dehumidifier

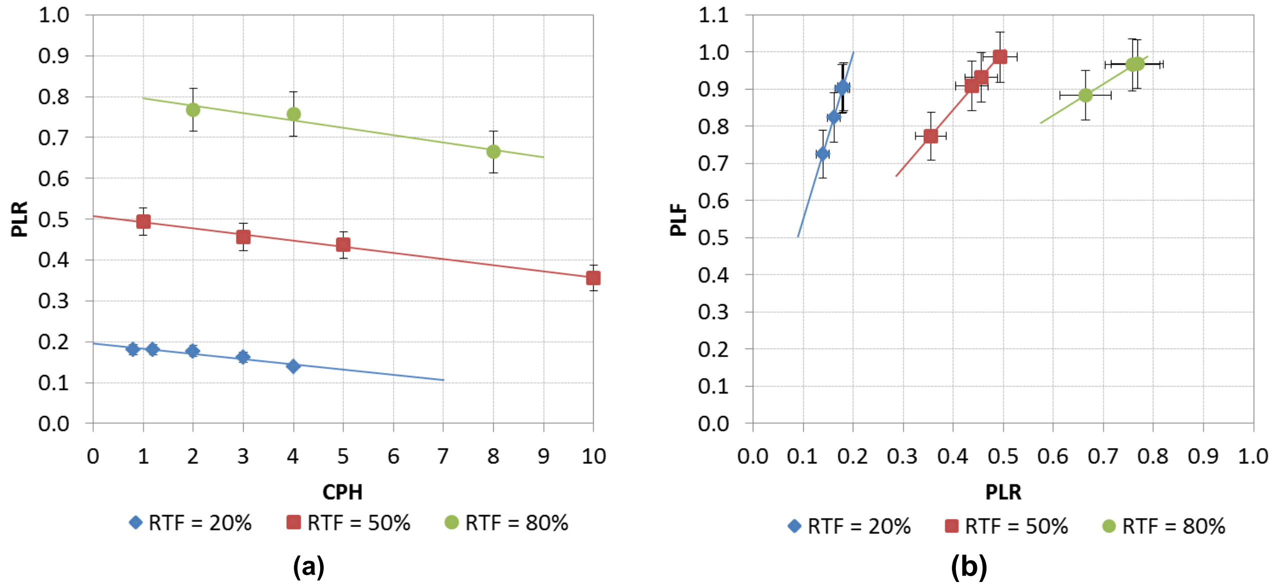

Figure 18. Part load performance plots for the Ultra-Aire 70H ducted dehumidifier

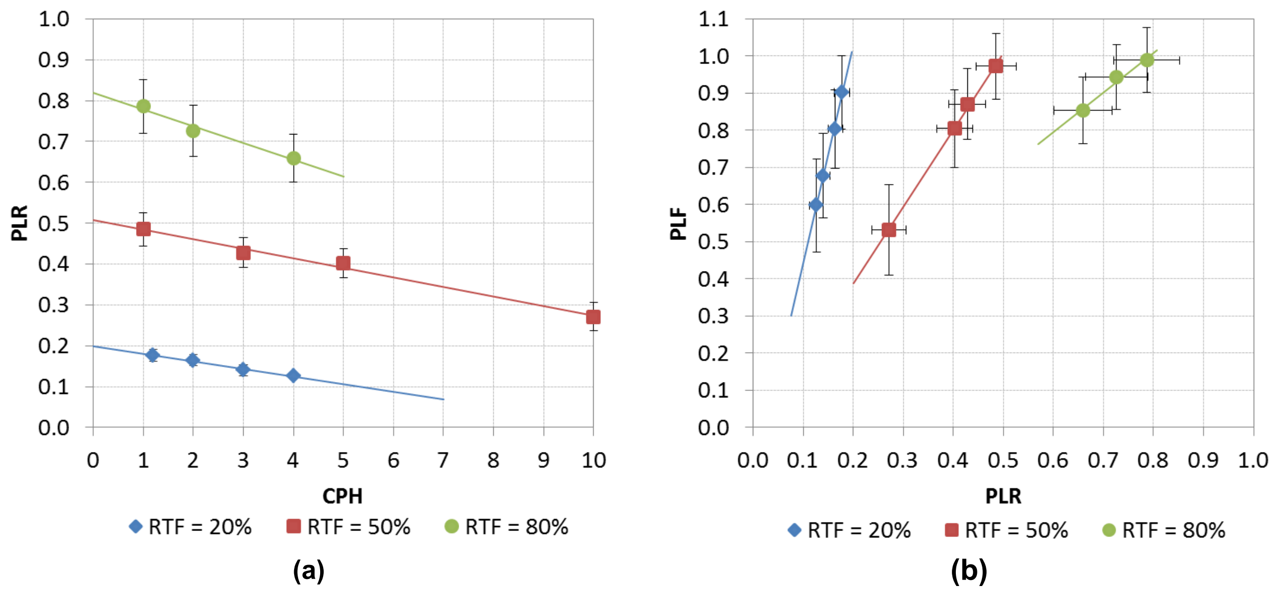

Figure 19. Part load performance plots for the GE ADER65LP standalone dehumidifier

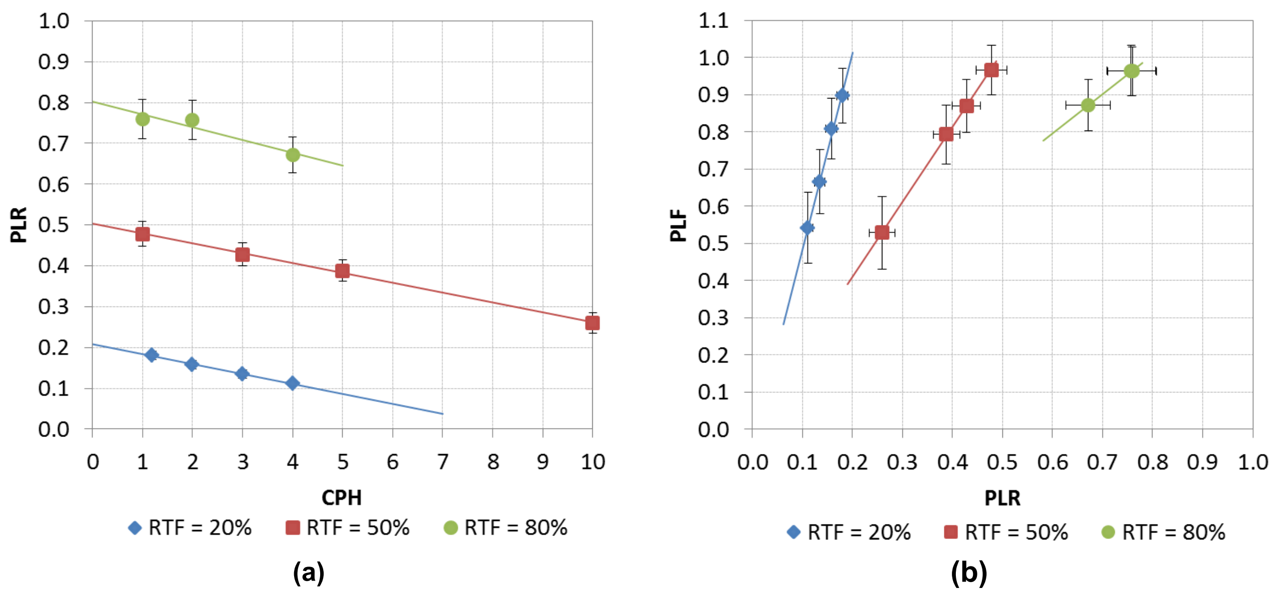

Figure 20. Part load performance plots for the Soleusair SG-DEH-45-1 standalone dehumidifier

Appendix D: Dehumidifier PLF Curves

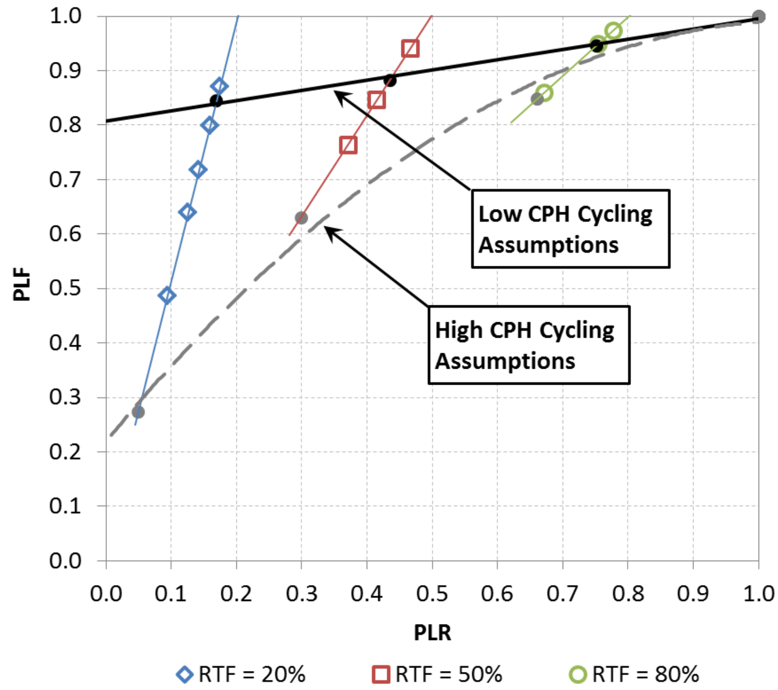

Figure 21. PLF performance curves for the Ultra-Aire XT150H ducted dehumidifier

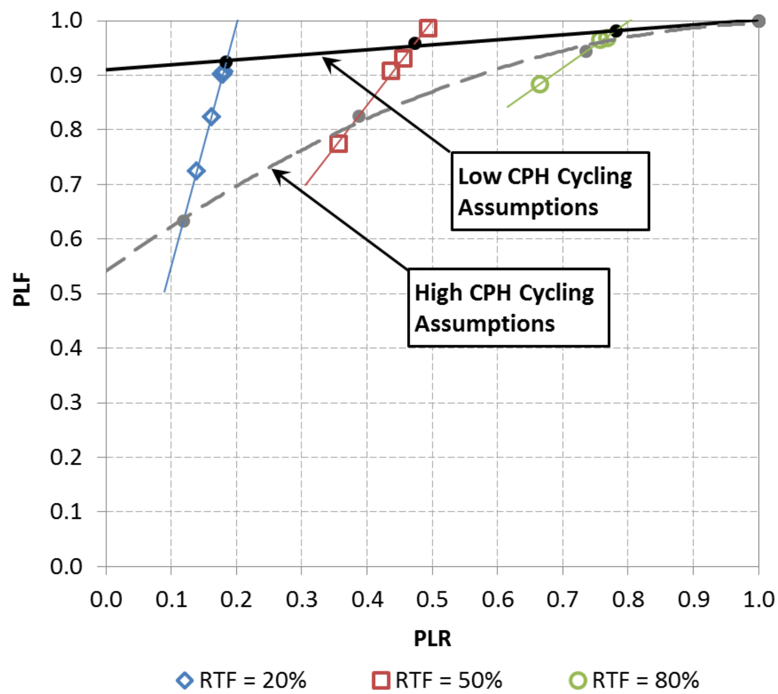

Figure 22. PLF performance curves for the Ultra-Aire 70H ducted dehumidifier

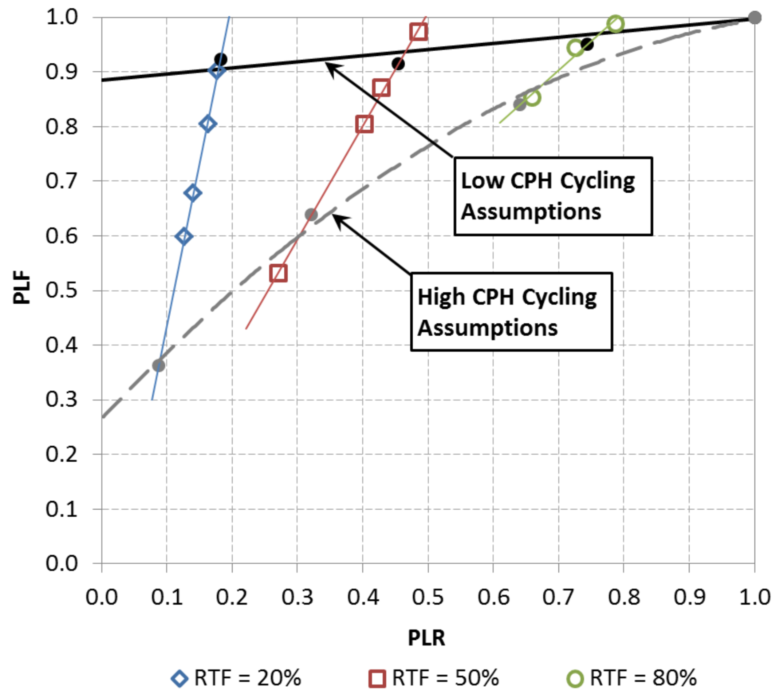

Figure 23. PLF performance curves for the GE standalone dehumidifier

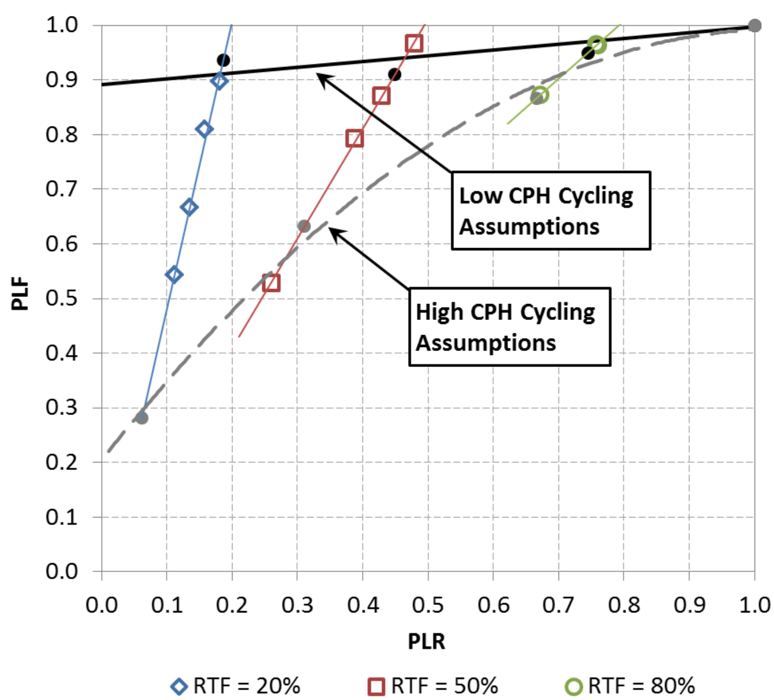

Figure 24. PLF performance curves for the Soleusair SG-DEH-45-1 standalone dehumidifier